

## Experimental Investigation on Thermal Diffusion in Ternary Hydrocarbon Mixtures

S. A. Mousavi<sup>1</sup>, T. Yousefi<sup>2</sup> and Z. Saghir<sup>3</sup>

**Abstract:** The main goal of this study was to investigate the thermal diffusion in ternary hydrocarbon mixtures composed of 1, 2, 3, 4 Tetrahydronaphtalene (THN)-Isobutylbenzene (IBB)-Dodecane (C12) with mass fractions of 80/10/10, 70/10/20, and 60/10/30 at mean temperature of 25 °C. Optical interferometry technique with Mach-Zehnder arrangement was used to conduct the experiments. The mixture was placed in a convectionless cell which was heated from above. The results for the mixture with mass fraction of 80/10/10 were in a good agreement with the corresponding benchmark values. Finally, the Soret coefficient for the other two mixtures have been proposed.

**Keywords:** Thermal diffusion, interferometry, Mach-Zehnder.

### 1 Introduction

In oil reservoirs in depth of 5-Km the segregation of the components in hydrocarbon mixtures is affected by pressure, Fickian diffusion, and thermal diffusion due to the geothermal gradient [Ghorayeb, Firoozabadi and Anraku (2003)]. Thermal diffusion or Soret effect is defined as dissociation of components in a multicomponent liquid mixture due to the presence of temperature gradient in the liquid. The competition of these three effects can lead to unusual distribution of the species in the vertical hydrocarbon wells. [Ghorayeb, Firoozabadi and Anraku (2003)] measured temperature, pressure, and composition in a gas field and found an unusual distribution of species where the denser fluid mixture floats motionless on top of the lighter mixture. In other words the density decreases with depth. The reason of such unusual distribution is migration of the denser components towards the cold side in the well (placed in a more elevated location) which is caused by thermal diffusion. The importance of the Soret effect in oil industry motivated researchers to study concentration distribution in hydrocarbon mixture affected by Soret effect. Rahman et al. [Rahman and Saghir (2014)] reviewed the experimental and theoretical methods of investigating Soret effect in liquid mixtures used in past. The experimental methods of Soret studies are mainly categorized into two groups of techniques according to the presence of convective motions. These two groups are named convective coupling methods and convectionless methods. In the first group the segregation of the components are driven by natural convection and Soret effect while in

---

<sup>1</sup> Ryerson University, Toronto, ON, Canada

<sup>2</sup> Ryerson University, Toronto, ON, Canada

<sup>3</sup> Ryerson University, Toronto, ON, Canada

the convectionless techniques motions in the mixture must be avoided and the separation of the mixture components occurs due to Soret effect alone.

In terrestrial condition because of the gravity force, natural convection in a system being heated from one side is unavoidable. In 1938 a setup was introduced by Clusius et al. [Clusius and Dickel (1938)] that took advantage of the gravity in segregation of the components in a multicomponent mixture. This set up was named thermogravitational column (TGC) or Clusius-Dickel column. The original column consisted of two concentric cylinders. The temperature of the inner cylinder was higher than the outer one and a gaseous mixture was trapped between the two cylinders. Because of thermal diffusion effect some components move towards the hot side and some travel towards the cold side. Then the lighter components float on top of the heavier ones and a concentration gradient is established between top and bottom of the column. This technique was used in hydrocarbon mixtures for the first time by Danby et al. [Danby, Lambert and Mitchell (1956)]. Rayleigh-Bénard Configuration [Chandrasekhar (1961)] is another convective coupling technique where the convective motions and Soret effect are induced by heating from below.

The heating from above configuration is applied in convectionless systems in order to prevent convective motions. A standard Soret cell consists of a cubic cavity bounded with copper blocks at top and bottom of it. The lateral walls are made of materials with very low conductivity to avoid horizontal temperature gradients. The sample mixture placed in the cavity is heated from above and the separation of the components commences. The denser component migrates towards the cold side which is the bottom side. Consequently, the system remains hydrostatically stabled.

Because of non-intrusive nature of the interferometry techniques, they are very popular in studying the convectionless techniques. Rahman and Saghir [Rahman and Saghir (2013)] used ground based interferometry technique with Mach-Zehnder arrangement to measure Soret coefficient of binary hydrocarbon mixtures placed in a Soret cell. One laser source with wavelength of 632.8 nm was used in the Mach-Zehnder interferometer. Ahadi et al. [Ahadi, Van Varenbergh and Saghir (2013)] investigated Soret effect in ternary hydrocarbon mixture THN, IBB, and C<sub>12</sub> with mass fraction of 10/80/10 at mean temperature of 25 °C. A Soret cell was used and experiments were performed in space using Mach-Zehnder interferometer with two laser sources with different wavelengths.

Although the Soret coefficient of ternary mixtures composed of THN, IBB, and C<sub>12</sub> at some compositions has been measured so far and the corresponding benchmark values are proposed [Bou-Ali, Ahadi, Alonso de Mezquia et al. (2015)] but still there are missing information about some mass fractions. To the best of our knowledge, there is no database provided for mass fractions of 60/10/30 and 70/10/20. The main goal of the current study is to measure Soret coefficients of these two compositions. Ground based interferometry technique with Mach-Zehnder arrangement was used to conduct the experiments.

## **2 Experimental section**

The ternary fluid mixtures used in the present were composed of THN, IBB, and C<sub>12</sub> at 25 °C. Three mass fractions were tested: 80/10/10, 70/10/20, and 60/10/30. The first

mixture with 80% THN was studied previously by other research groups and a benchmark has been proposed for the corresponding Soret coefficients [Bou-Ali, Ahadi, Alonso de Mezquia et al. (2015)]. This composition was investigated again in the current study in order to validate the experimental setup.

The cell containing the mixture is shown in Figure 1. A glass wall with a cubic cavity in middle of it is clamped between two nickel-plated copper blocks. The contact surfaces between the copper blocks and the window are sealed with O-rings. Laser beams traverse the mixture through the glass window. The cavity is filled with the testing mixture through filling channels. The copper blocks and glass window are covered and insulated with Teflon Polytetrafluoroethylene (PTFE). The copper blocks are heated independently by Peltier modules. The lower and upper boundaries play the role of cold and hot side respectively. The applied temperature gradient between these sides is 1 K/mm. the height of the cavity is 2.5 mm.

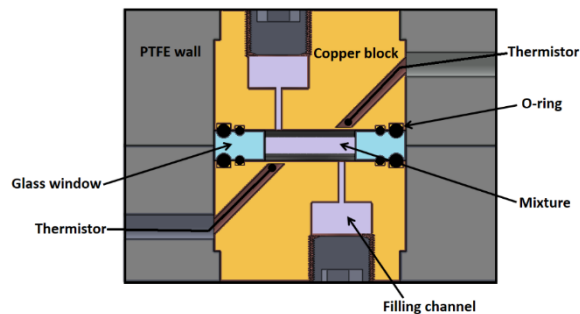


**Figure 1:** Soret cell

After filling the cell and sealing the filling channels it is installed on the optic bench with Mach-Zehnder arrangement shown in Figure 2.

Two lasers with wavelengths of 670 nm and 935 nm were used to monitor the sample in the cell. A beam splitter redirects the second laser beam to the Mach-Zehnder interferometer. Shutters installed next to each laser source operate in a way that the beam of one of the lasers passes through the Mach-Zehnder at a time. A spatial filter expands the emitted beam and a plano-convex lens collimates the expanded beam. Thereafter, the collimated beam is divided into two beams by a beamsplitter. One beam traverse the Soret cell and the second one passes through undisturbed environment and it is called the reference beam. Both beams are recombined again at the second beam splitter and then focused on a camera. The optical path difference between the beams constructs a fringe pattern shown on screen.

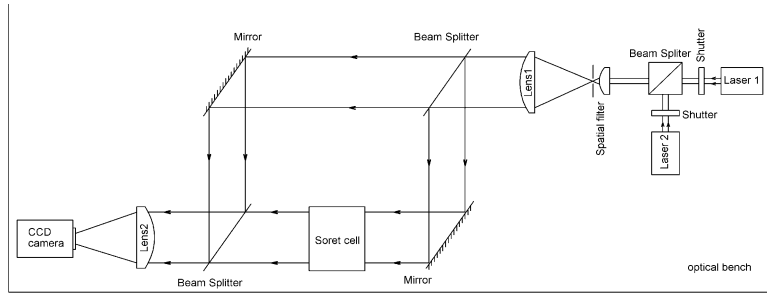


**Figure 2:** Mach-Zehnder interferometer setup

### 3 Data analysis

The data processing methodology used in the present study has been explained in ref. [Ahadi, Van Varenbergh and Saghir (2013)]. A sample fringe pattern captured in a random time during the experiment is shown in Figure 3. The low quality of the fringes near the hot and cold walls due to beam deflection must be cropped out. The possible heat fluxes near the lateral walls can cause convective motions in such regions. However the center of the cell is assumed to be convectionless. Thus, a rectangular crop is used in center of the cell and the outside of the rectangular is cropped out.

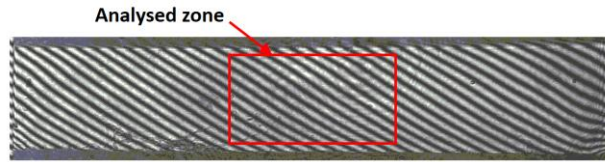


**Figure 3:** Fringe pattern

The changes of refractive index,  $\Delta n$ , can be calculated as follows:

$$\Delta n(x, y, t_i) = \frac{\lambda}{2\pi L} \Delta \varphi(x, y, t_i) \quad (1)$$

where  $\lambda$  stands for the wavelength of laser source,  $L$  represents the optical length of the sample, and  $\Delta \varphi$  is phase change due to the changes in refractive index.  $\Delta \varphi$  is obtained by using Fast Fourier Transform (FFT) [Ahadi, Van Varenbergh and Saghir (2013)]. Having two lights with different wavelengths and the corresponding phase changes, two different variation of refractive index can be found. In addition, the variation of the index of refraction is caused by the changes of temperature and concentration:

$$\Delta n_1(x, z) = \left( \frac{\partial n_1}{\partial T} \right) \Delta T(x, z) + \left( \frac{\partial n_1}{\partial C_1} \right) \Delta C_1(x, z) + \left( \frac{\partial n_1}{\partial C_2} \right) \Delta C_2(x, z) \quad (2)$$

$$\Delta n_2(x, z) = \left( \frac{\partial n_2}{\partial T} \right) \Delta T(x, z) + \left( \frac{\partial n_2}{\partial C_1} \right) \Delta C_1(x, z) + \left( \frac{\partial n_2}{\partial C_2} \right) \Delta C_2(x, z) \quad (3)$$

where  $\Delta n_1$  and  $\Delta n_2$  are changes of refractive index corresponding to the two different wavelengths and calculated from Eq. (1).  $\left( \frac{\partial n}{\partial T} \right)$  and  $\left( \frac{\partial n}{\partial C} \right)$  are called contrast factors and

they are provided in ref. [Yahya and Saghir (2015)] and [Sechenyh, Legros and Shevtsova (2013)] for different wavelengths and compositions.  $\Delta C_1$  and  $\Delta C_2$  are changes of concentration of component one and two respectively.

After applying the temperature gradient, it takes few minutes approximately three minutes to reach thermal steady state while it takes about 300 minutes to establish a steady concentration field. It means that the contribution of the concentration in changes of the refractive index during thermal time is negligible. Thus Eqs. (2) and (3) are reduced as follows:

$$\Delta n_1(x, z) = \left( \frac{\partial n_1}{\partial T} \right) \Delta T(x, z) \quad (4)$$

$$\Delta n_2(x, z) = \left( \frac{\partial n_2}{\partial T} \right) \Delta T(x, z) \quad (5)$$

Temperature field is obtained from either of the above last equations. The changes of refractive index after thermal time is only caused by concentration changes:

$$\Delta n_1(x, z) = \left( \frac{\partial n_1}{\partial C_1} \right) \Delta C_1(x, z) + \left( \frac{\partial n_1}{\partial C_2} \right) \Delta C_2(x, z) \quad (6)$$

$$\Delta n_2(x, z) = \left( \frac{\partial n_2}{\partial C_1} \right) \Delta C_1(x, z) + \left( \frac{\partial n_2}{\partial C_2} \right) \Delta C_2(x, z) \quad (7)$$

$\Delta C_1$  and  $\Delta C_2$  are obtained from Eqs. (6) and (7) and the concentration changes of the third component is found from  $\Delta C_1 + \Delta C_2 + \Delta C_3 = 0$ .

## 4 Results

The experiment on each mixture was performed three times in order to evaluate the repeatability of the technique. Temperature and concentration profiles for the three tested mixtures with different mass fractions were obtained experimentally by interferometry technique. Having the concentration contour, the migration direction of each component can be determined. The concentration difference between the cold and hot side of the cell was used to measure Soret coefficient.

### 4.1 Temperature profile

After applying the temperature gradient, the steady state temperature profile established in almost three minutes. The linear distribution of temperature profile between top and bottom side of the cell is depicted in Figure 4. Absence of horizontal temperature gradient shows the pure heat conduction in the mixture which is desirable because it does not induce convective motions. The temperature on the top and bottom lines vary based on the location of the cropped zone.

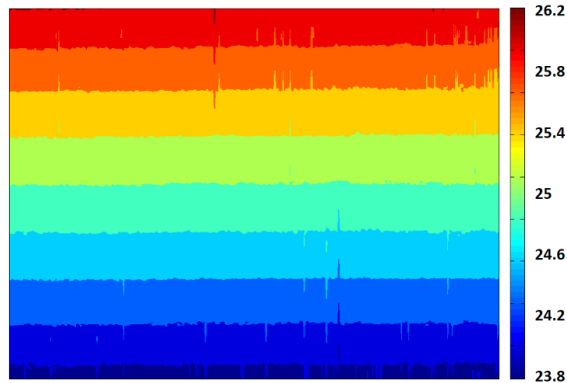


**Figure 4:** Temperature distribution in the cropped zone

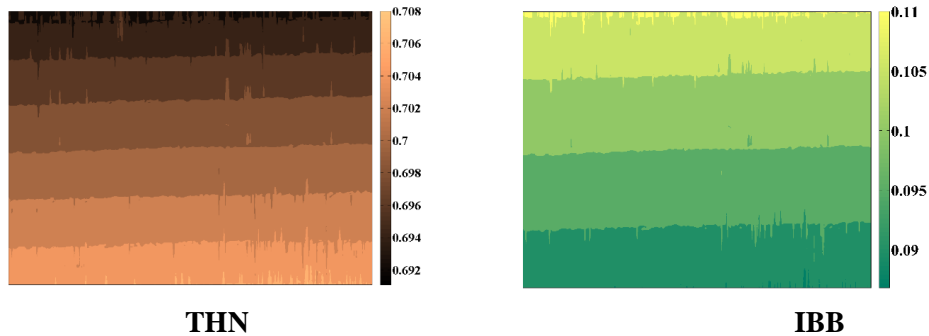
#### 4.2 Concentration field and Soret coefficient

Figure 5 shows the concentration fields of THN and IBB in the mixture with mass fraction of 70/10/20 after 250 minutes. The dimensions of the illustrated areas are equal with those for the cropped zone which are smaller than the actual dimensions of the cavity. As seen, THN and IBB migrated towards the cold and hot side respectively. The maximum concentration difference ( $C_{hot} - C_{cold}$ ) for all mass fractions are presented in Table 1. The maximum separation occurred after approximately 300 minutes.

Eq. (8) has been used to determine Soret coefficients.

$$S_T = -\frac{\Delta C_{\max}}{\Delta T} \quad (8)$$

The measured  $s_T$  and the benchmark values are presented in Table 2. The benchmark values are proposed in ref. [Bou-Ali, Ahadi, Alonso de Mezquia et al. (2015)] for the mixture with mass fraction of 80/10/10. The agreement between the obtained results in the present study and the benchmark values shows the validity of the technique.



**Figure 5:** Concentration distribution after 250 minutes

**Table 1:** Maximum separation and corresponding temperature gradient

mass fraction	80/10/10	70/10/20	60/10/30
$\Delta C_{\max}^{THN} \times 10^{-3}$	-1.98	-4.14	-3.92
$\Delta C_{\max}^{IBB} \times 10^{-3}$	0.64	2.75	2.71
$\Delta T (K)$	1.59	1.58	1.71

**Table 2:** Benchmark and measured Soret coefficient

mass fraction	$S_T^{THN} \times 10^{-3} [K^{-1}]$	$S_T^{IBB} \times 10^{-3} [K^{-1}]$	$S_T^{C12} \times 10^{-3} [K^{-1}]$
80/10/10 (benchmark)	1.4±0.16	-0.57±0.26	-0.83±0.10
80/10/10(measured)	1.24±0.09	-0.40±0.075	-0.84±0.083
70/10/20	2.66±0.051	-1.76±0.06	-0.90±0.055
60/10/30	2.29±0.046	-1.58±0.05	-0.71±0.047

## 5 Conclusion

In the present study, thermal diffusion in ternary hydrocarbon mixtures was studied experimentally. The Soret cell containing the mixture was installed on an optical bench in a Mach-Zehnder interferometer. Two laser sources with different wavelengths were used and the fringe patterns were analysed using 2D- FFT method. The temperature distribution in the mixture was found to be linear with no horizontal temperature gradient. The concentration distribution for each component was obtained and the concentration difference between the hot and cold side of the cavity was used to calculate the Soret coefficient. A table of proposed Soret coefficient was provided. The results were in a good agreement with the benchmark values. It is the first report on the Soret coefficient for mass fraction of 70/10/20 and 60/10/30.

**Acknowledgments:** The authors acknowledge the financial support of the Canadian Space Agency, The National Science and Engineering Council and the European Space Agency.

## References

- Ahadi, A.; Van Varenbergh, S.; Saghir, M. Z.** (2013): Measurement of the Soret coefficients for a ternary hydrocarbon mixture in low gravity environment. *Journal of Chemical Physics*, vol. 138, no. 20, pp. 204201.
- Bou-Ali, M. M.; Ahadi, A.; Alonso de Mezquia, D.; Galand, Q.; Gebhardt, M. et al.** (2015): Benchmark values for the Soret, thermodiffusion and molecular diffusion coefficients of the ternary mixture tetralin+isobutylbenzene+n-dodecane with 0.8-0.1-0.1 mass fraction. *European Physical Journal E*, vol. 38, no. 4, pp. 1-6.

**Chandrasekhar, S.** (1961): *Hydrodynamic and hydromagnetic stability*. Oxford University Press.

**Clusius, K.; Dickel, G.** (1938): Neues verfahren zur gasentmischung und isotopentrennung. *Naturwissenschaften*, vol. 26, no. 33, pp. 546-546.

**Danby, C. J.; Lambert, J. D.; Mitchell, C. M.** (1956): Separation of hydrocarbon isomers by thermal diffusion. *Nature*, vol. 177, pp. 1225-1226.

**Ghorayeb, K.; Firoozabadi, A.; Anraku, T.** (2003): Interpretation of the unusual fluid distribution in the Yufutsu gas-condensate field. *SPE Journal*, vol. 8, no. 2, pp. 114-123.

**Rahman, M. A.; Saghir, M. Z.** (2013): Ground based measurement and theoretical calculation of Soret coefficient of binary hydrocarbon mixtures. *Experimental Thermal and Fluid Science*, vol. 49, pp. 31-39.

**Rahman, M. A.; Saghir, M. Z.** (2014): Thermodiffusion or soret effect: historical review. *International Journal of Heat and Mass Transfer*, vol. 73, pp. 693-705.

**Sechenyh, V. V.; Legros, J. C.; Shevtsova, V.** (2013): Optical properties of binary and ternary liquid mixtures containing tetralin, isobutylbenzene and dodecane. *Journal of Chemical Thermodynamics*, vol. 62, pp. 64-68.

**Yahya, M.; Saghir, M. Z.** (2015): Prediction and experimental measurement of refractive index in ternary hydrocarbon mixtures. *Journal of Chemical & Engineering Data*, vol. 60, no. 8, pp. 2329-2342.